

MICROSTRUCTURE OF METAL-MATRIX COMPOSITES REINFORCED BY CERAMIC MICROBALLOONS

MIKROSTRUKTURA KOMPOZITOV S KOVINSKO OSNOVO, OJAČANO S KERAMIČNIMI MIKROKROGLICAMI

Imre Norbert Orbulov, Kornél Májlinger

Department of Materials Science and Engineering, Budapest University of Technology and Economics, Bertalan Lajos utca 7.,
1111, Budapest, Hungary
orbulov@eik.bme.hu, orbulov@gmail.com

Prejem rokopisa – received: 2011-12-03; sprejem za objavo – accepted for publication: 2012-02-06

Metal-matrix composites reinforced by ceramic hollow microspheres were produced as special porous metals, called metal-matrix syntactic foams (MMSFs). In this paper the microstructure of the ceramic hollow microspheres as reinforcing elements is investigated in connection with the production of MMSFs with the pressure infiltration. SL150- and SL300-type ceramic microspheres from Envirospheres Ltd (Australia) were investigated. They contained various oxide ceramics, mainly Al_2O_3 and SiO_2 . The chemical composition and the microstructure of the microspheres had a strong effect on their infiltration characteristics; therefore, in the view of the MMSF production it was very important to know microstructural details about the microspheres. Due to this energy-dispersive X-ray spectroscopy, maps were recorded from the cross-sections of the microspheres' walls. The results showed that the Al_2O_3 and SiO_2 distribution were not equal; the Al_2O_3 phase was embedded in the surrounding mullite, while the SiO_2 phase occurred in the form of needles. Line energy-dispersive X-ray spectroscopy measurements were performed in order to investigate the possible reaction between different aluminium alloy matrices and the ceramic microspheres. The results showed that, due to an uneven distribution of Al_2O_3 , rich particles of the molten aluminium could reduce the SiO_2 rich parts of the microspheres and the walls of the hollow microspheres became damaged and degraded. This chemical reaction between the microspheres and the walls could make the infiltration easier, but the resulting mechanical properties will be reduced due to the damaged microsphere walls.

Keywords: microsphere, microballoon, energy dispersive X-ray spectroscopy, metal matrix syntactic foam, metal matrix composite

Kompoziti s kovinsko osnovo, ojačano s keramičnimi votlimi mikrokroglicami, so bili izdelani kot posebna porozna kovina z nazivom sintaktična pena s kovinsko osnovo (MMSF). V tem članku je opisana raziskava mikrostrukture keramičnih votlih mikrokroglic v povezavi z izdelavo MMSF z infiltracijo pod tlakom. Preiskovane so bile SL150- in SL300-keramične mikrokroglice proizvajalca Envirospheres Ltd (Avstralija). Vsebujejo različne keramične okside, večinoma Al_2O_3 in SiO_2 . Kemijska sestava in mikrostruktura mikrokroglic imata velik vpliv na sposobnost njihove infiltracije, zato je z vidika izdelave MMSF pomembno poznati podrobnosti mikrostrukture teh mikrokroglic. Zaradi tega je bila na prerezu stene mikrostrukturnih kroglic posneta razporeditev elementov z energijsko disperzijsko spektroskopijo. Rezultati kažejo, da razporeditev Al_2O_3 in SiO_2 ni enaka: Al_2O_3 -faza je vgrajena v obkrožajoči mulit, medtem ko se SiO_2 -faza pojavlja v obliki igel. Da bi preiskali morebitne reakcije med osnovo iz različnih aluminijevih zlitin in keramičnimi mikrokroglicami, je bila izvršena linijska energijsko disperzijska rentgenska spektroskopija. Rezultati so pokazali, da zaradi neenakomerne razporeditve z Al_2O_3 bogati delci v staljenem aluminiju lahko reducirajo s SiO_2 bogata področja mikrokroglic, in stene votlih mikrokroglic postanejo poškodovane in degradirane. Kemijske reakcije med mikrokroglicami in stenami lahko olajšajo infiltracijo, vendar pa se mehanske lastnosti poslabšajo zaradi poškodovanih sten mikrokroglic.

Ključne besede: mikrokroglice, mikrobalooni, energijsko disperzijska rentgenska spektroskopija, pena, skladna s kovinsko osnovo, kompozit s kovinsko osnovo

1 INTRODUCTION

Nowadays metallic foams are more and more important and this is confirmed by the increasing number of papers published on this topic. The 'conventional' metallic foams, which contain only metallic and gas phases, are widely covered by the literature. However, there are still unsolved problems, for example the foaming process of the foams^{1,2}. The metallic foams belong to a special class that also satisfies the definition of the particle-reinforced metal-matrix composites. These are the metal-matrix syntactic foams (MMSFs). They were first produced in the 1990s. The MMSFs have numerous promising applications, such as covers, hulls, castings, or they can be used in the automotive and electromechanical industry sectors because of their high-energy absorbing and

damping capabilities. In these porous materials the porosity is ensured by incorporating ceramic hollow microspheres³. The microspheres are commercially available and they mainly contain various oxide ceramics^{4,5}. The quality of the microspheres has a strong effect on the mechanical and other properties of the foams. The behavior of the foams has been widely studied.

The most important properties of the foams are the compressive strength and the absorbed energy. Wu et al. examined the effects of the microballoon size on the compressive strength. They found that smaller microspheres ensure higher compressive strength because they contain fewer flaws in their microstructure than the larger ones. The damage propagation of the foams was also investigated. The fracture was initialized in the cor-

ners of the specimens by the shearing of the microspheres⁶. Rohatgi et al. also investigated the size effect of the microspheres, but not only in view of the compressive strength, but in view of infiltration, too. Their measurements showed that larger microspheres can be infiltrated easier⁷. Palmer et al. proved that larger microspheres contain more porosity in their walls and more flaws in their microstructure than the smaller ones⁸. The results of the performed upsetting tests were compared to the other research on this topic. The conclusions were the same^{9,10}. Balch et al. performed a special upsetting test. The loading was applied in small steps and after each test, X-ray or neutron-diffraction measurements were carried out. The main aim of the work was to investigate the load transfer from the matrix to the microspheres. They found a chemical reaction between the microspheres and the matrix materials, which has a detrimental effect on the load transfer and, through that, on the mechanical properties of the foams¹¹. In their previous work Balch et al. found that the microspheres have at least the same importance in the syntactic foams as the matrix material. The fracture strength and the yield strength of the matrix determine the failure stress of the syntactic foams. Therefore, the investigation of the microstructure and the quality of the microspheres is very important⁹. In addition to the compressive strength, other mechanical properties, such as the tensile strength, or the hardness of the syntactic foams were investigated^{12,13}. The sliding behavior of the syntactic foams was also examined because the ceramic microspheres have high hardness and therefore the composites show a better wear behaviour than the pure matrix^{14,15}.

As it can be seen in the previous paragraph, the quality and chemical composition of the microspheres influence many properties of the syntactic foams. And they also have a strong influence on the production of the syn-

tactic foams. The foams are usually produced by the mixing technique and gravitational casting or by the pressure infiltration. In all these cases the contact angle between the ceramic microspheres and the metal matrix has a detrimental effect on the infiltration characteristics and on the threshold pressure (in the case of pressure infiltration)¹⁶⁻¹⁸. The contact angle is influenced by many parameters like the chemical composition and the possible reaction between the reinforcement and the matrix material. Therefore, the microspheres should be precisely investigated on the microstructure's scale.

The ultimate method for this purpose is the scanning electron microscopy and the energy-dispersive X-ray spectroscopy (EDS). EDS is sensitive to the chemical composition and able to investigate a point, a line or even an area. These possibilities give extremely good opportunities for acquiring detailed information about the microstructure of the microspheres and about the distribution of their constituents. According to the published works mentioned above, the main aim of this work was to investigate the microstructure and the distribution of the constituents in the ceramic hollow microspheres and to investigate the interface between different aluminium-alloy matrices and the ceramic microspheres in order to provide information about the metal-matrix syntactic foam production and their expectable mechanical behaviour.

2 MATERIALS AND METHODS

The investigated materials were the SL150- and SL300-type microspheres provided by Envirospheres Ltd (Australia)⁴. Their main parameters are listed in **Table 1**. The phase composition was determined by X-ray diffraction measurements. For this purpose a Phillips X-Pert-type diffractometer with 35-mA cathode heating current

Table 1: Morphological properties and the phase constitution of the applied hollow ceramic spheres

Tabela 1: Morfološke značilnosti fazne sestave uporabljenih votlih keramičnih kroglic

Type	Average diameter	Size range	Specific surface	Al ₂ O ₃	Amorphous SiO ₂	Mullite	Quartz	Other
	(μm)	(μm)	(μm^{-1})					
SL150	100	56–183	0.060	30–35	45–50	19	1	<i>bal.</i>
SL300	150	101–330	0.040					

Table 2: Calculated and measured density and porosity values of the MMSFs³

Tabela 2: Izračunane in izmerjene vrednosti za gostoto in poroznost MMSF³

Specimen	Density (g cm ⁻³)		Porosity (%)		
	Theoretical	Measured	Particle	Matrix	Total
Al99.5-SL150	1.34	1.43	50.9	-6.2	44.7
Al99.5-SL300	1.42	1.52	48.2	-7.2	41.0
AlSi12-SL150	1.32	1.31	50.9	1.1	52.0
AlSi12-SL300	1.40	1.37	48.2	1.9	50.1
AlMgSi1-SL150	1.34	1.52	50.9	-13.4	37.5
AlMgSi1-SL300	1.42	1.57	48.2	-10.5	37.7
AlCu5-SL150	1.37	1.53	50.9	-11.6	39.3
AlCu5-SL300	1.44	1.62	48.2	-12.2	36.0

and a copper anode (Cu K_{α} , $\lambda = 0.154186$ nm) with a 40-kV voltage were used. The rotating speed of the goniometer was $0.04^{\circ} \text{ s}^{-1}$. The Scanning Electron Microscope (SEM) tests were performed by a Phillips XL-30-type electron microscope equipped with an EDAX Genesis EDS analyzer. The ceramic microspheres were coated with carbon in order to put a conductive layer on them, but basically they were investigated in as-received condition. The excitation was 15 kV and EDS maps were recorded from the surface of the microspheres. Five typical microspheres from each SL-type microsphere group were investigated.

Later the microspheres were incorporated in pure aluminium (Al 99.5), aluminium-silicon (AlSi12), aluminium-magnesium-silicon (AlMgSi) or aluminium-copper (AlCu5) alloys to create MMSFs. The foams were designated according to their matrices and reinforcement. For example, Al99.5-SL150 denotes a pure aluminium-matrix syntactic foam with an SL15-microsphere reinforcement. The volume fraction of the microspheres was maintained at a relatively high volume fraction (≈ 60 %) level and the production method is described, in details, elsewhere³. The density and the porosity values of MMSFs are listed in **Table 2**, while the chemical compositions of MMSFs are shown in **Table 3**. In **Table 2** theoretical density and particle porosity were calculated from the geometrical parameters of the microspheres. The matrix porosities were calculated as the difference between the theoretical and the measured density divided by the theoretical density. The negative matrix porosity refers to the infiltrated microspheres (the particle porosity should be decreased). However, the values of the matrix porosity were always below 8 %, so the infiltration can be qualified as good enough. The values of **Table 3** were determined with the XRD measurements described

above. EDS line measurements were carried out on the foams to characterize the elemental distribution at the interfaces, where the hollow microspheres are in contact with the matrix. All EDS-line analyses were performed on metallographically polished surfaces, and the preparation steps for the EDS analysis with an automatic grinding / polishing machine are listed in **Table 4**. The excitation voltage for the EDS analysis was 20 kV. The line EDS measurement started on the matrix material and crossed the wall of a hollow sphere. One hundred points were measured along each line; each point was excited for 20 s with a 35- μs detector acquisition rate.

3 RESULTS AND DISCUSSION

3.1 Investigation of the microspheres' walls (map EDS measurements)

In **Figure 1** a typical site from the outer surface of an SL150-type microsphere is shown, while in **Figure 2**, a SEM micrograph from the cross-section of a microsphere in an Al99.5-matrix foam sample is presented. In both images needle-like structures can be clearly observed. They are densely situated and they do not have any distinguished direction. The different gray scale of the needles on the back-scattered electron (BSE) images indicates a somewhat different chemical composition. The needles are very small, their length is between 5 μm and 10 μm , while their diameter is smaller than 0.5 μm . EDS maps provide information that is much more useful than the single EDS spot measurements, because single spots can be largely effected by the surrounding matrix. This effect can be decreased, or avoided, with the EDS maps, which can show the distribution of the elements.

Because of this reason the EDS-map analyses were performed on the cross-sections of the microspheres to

Table 3: Phase constitution of aluminum-matrix syntactic foams according to the XRD measurements (in mass fractions, w/%)

Tabela 3: Fazna sestava pen, skladnih s kovinsko osnovo, izvršena z XRD-meritvami (v masnih deležih, w/%)

Specimen	Al	Si	Mullite	α -Al ₂ O ₃	γ -Al ₂ O ₃	Amorph.	CuAl ₂
Al99.5-SL150	67	8	11	3	11	0	-
Al99.5-SL300	78	0	11	0	0	11	-
AlSi12-SL150	72	7	13	0	0	8	-
AlSi12-SL300	72	7	12	0	0	8	-
AlMgSi1-SL150	60	7	8	0	25	0	-
AlMgSi1-SL300	60	6	6	0	28	0	-
AlCu5-SL150	60	6	8	8	12	0	6
AlCu5-SL300	60	5	10	7	12	0	6

Table 4: Sample-preparation steps for the EDS analysis with an automatic grinding / polishing machine

Tabela 4: Stopnje priprave vzorcev za EDS-analizo z avtomatskim brusilno-polirnim sistemom

Abrasive material	Duration of grinding/polishing (min)	Grinding/polishing force (N)	Rotation speed (r/min)	Rotation direction
P 320 SiC	1	22	220	counter
6 μm diamond	15	27	150	counter
3 μm diamond	6	27	150	counter
0.05 μm SiO	3	27	125	compliance

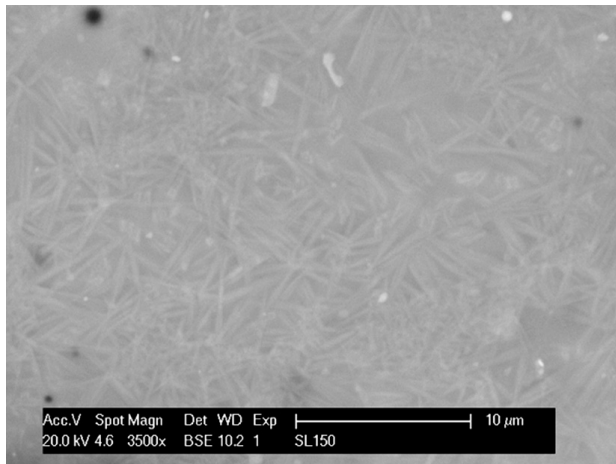


Figure 1: SEM image from the surface of an SL150-type ceramic hollow microsphere

Slika 1: SEM-posnetek površine SL150 votle keramične mikrokroglice

get additional information about the element distribution in a microsphere's wall. To illustrate this analysis, the EDS maps of an SL300-type microsphere are presented (**Figure 3**). It is important to emphasize that all of the other microsphere types (SL150 and SL300) showed the same features. **Figure 3a** shows a SEM image of the investigated surface. The needle-like structure is again very clear. **Figure 3b** shows the distribution of aluminium. It is evident that the needles contain more Al than the surrounding environment, but Al can be found everywhere, not only in the needles. From the XRD measurements it is also clear that Al_2O_3 and SiO_2 form mullite ($3\text{Al}_2\text{O}_3 \cdot 2\text{SiO}_2$), therefore – in accordance with the EDS map and **Table 1** – the wall of a microsphere is built up from the mixture of mullite and amorphous SiO_2 . This means that the distribution of Al_2O_3 is uneven; it can be found as a part of mullite in the wall and as

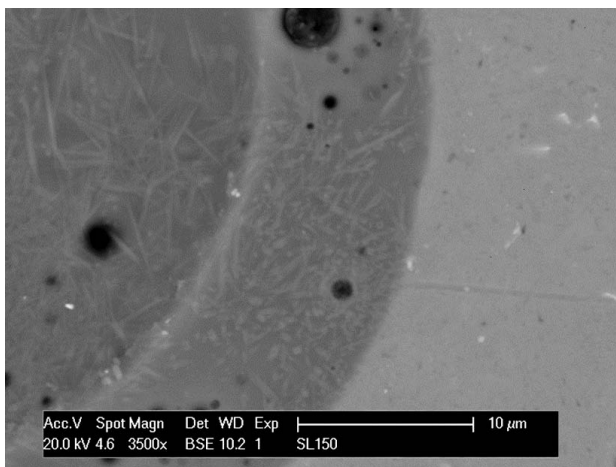


Figure 2: SEM image of the cross-section of an SL150-type ceramic hollow microsphere's wall

Slika 2: SEM-posnetek prečnega prereza stene SL150 votle keramične mikrokroglice

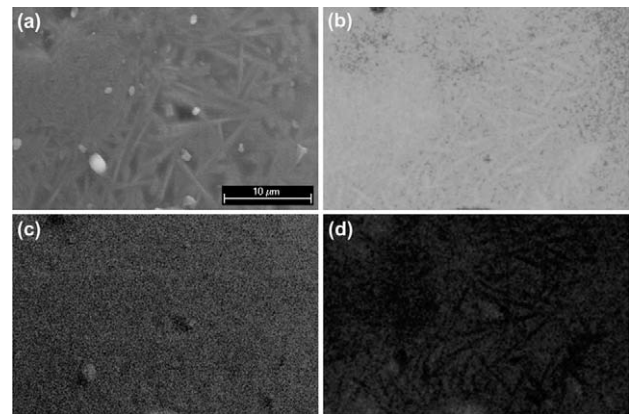


Figure 3: SEM image a) from the surface of an SL300-type microsphere and EDS maps of this area showing element distributions of: b) Al, c) O and d) Si

Slika 3: SEM-posnetek a) površine SL300 mikrokroglice in EDS posnetek razporeditve elementov: b) Al, c) O in d) Si

Al_2O_3 needles embedded in this wall matrix. **Figure 3d** definitely confirms this conclusion by showing the distribution of silicon. Si can be found everywhere on the surface (mainly amorphous SiO_2 mixed with mullite) except in the needles (the needles appear black in this picture). This indicates that the needles do not contain Si and, therefore, they are really Al_2O_3 needles. Finally, as it is expected, the oxygen distribution (in **Figure 3c**) is totally balanced; it is built in both Al_2O_3 and SiO_2 .

The analysis above shows the formation of the Al_2O_3 rich zones and it also indicates the presence of the amorphous SiO_2 rich zones. The amorphous SiO_2 is undesir-

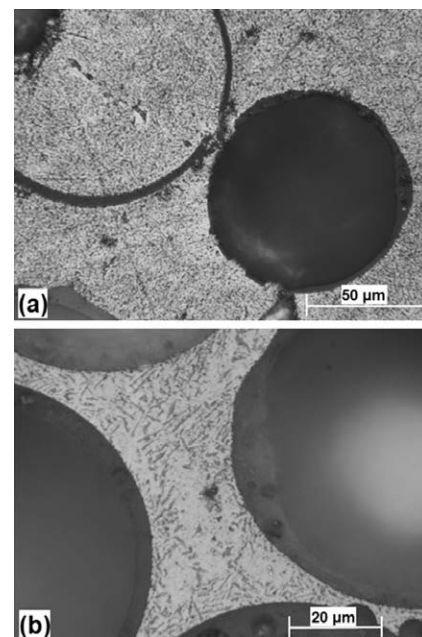


Figure 4: Micrographs of: a) damaged and b) undamaged microspheres in the a) Al99.5 and b) AlSi12 matrices

Slika 4: Mikrosposnetek: a) poškodovane in b) nepoškodovanih mikrokroglic v a) Al99,5 in b) AlSi12 osnovi

able, because – opposite to Al_2O_3 and mullite – the chemical stability of SiO_2 at an elevated temperature is not good enough. During the production of MMSFs the molten aluminium can reduce SiO_2 according to the following chemical reaction:



At first sight this reaction is advantageous, because it forms Al_2O_3 (with better properties) from amorphous SiO_2 . But this is a diffusion-controlled reaction leading to a degradation of the microspheres' walls as it is shown in **Figure 4a**. This indicates a drastic drop in the compressive strength and other mechanical properties as it was shown in the previous papers^{3,19,20}. As indicated by the XRD results of **Table 3**, the reaction mainly produced $\gamma\text{-Al}_2\text{O}_3$ and it took place only in the case of a pure aluminium matrix reinforced with the SL150- and SL300-type microspheres. In the case of the SL300-type microspheres the reaction was suppressed with a lower infiltration temperature. The infiltration temperature had a strong influence on the kinetics of the change reaction. That is why there was no reaction in the case of the Al99.5-SL300-type syntactic foams infiltrated at a lower (690 °C) temperature³. This indicates that there is a limit relating to the temperature. Above this temperature the reaction is intensive, but below the temperature limit, the reaction will not occur (for details see³). The reaction did not take place in the case of the AlSi12-matrix material, because the driving force of the diffusion-controlled chemical reaction is the Si difference between the molten matrix and the solid microspheres. In the case of the AlSi12 metal, the large Si content decreased the driving force; the reaction became suppressed and did not take place. The walls of the microspheres remained unharmed as it can be observed in **Figure 4b**. Most of $\gamma\text{-Al}_2\text{O}_3$ was found in the MMSFs with the AlMgSi1 matrix and the

above mentioned reaction also took place in the samples with the AlCu5 matrix. In the case of the MMSFs with the AlCu5 matrix, the thermodynamic conditions also enabled the formation of the CuAl_2 phase.

To summarize, the microspheres form the Al_2O_3 needles embedded in the mixture of the amorphous SiO_2 and mullite. The chemically reactive molten aluminium can damage the microspheres by reducing their amorphous SiO_2 -rich parts. This is undesirable with respect to mechanical properties.

3.2 Investigation of the interface layer between microspheres and the matrix

After a detailed examination of the microspheres' surfaces, the investigations of MMSFs were carried out.

First, EDS overview-map measurements were performed in the microsphere-matrix region of the MMSFs with different matrices. For example, in the case of an Al99.5 matrix with SL300 microspheres, the EDS-map results are shown in **Figure 5**. The area of the SEM image (**Figure 5a**) was investigated for the distribution of the alloying elements (**Figures 5b to 5d**). The microstructure of the matrix-grain boundaries formed after the solidification can be seen clearly in the concentration differences between aluminium (**Figure 5b**) and silicon (**Figure 5d**) in the EDS images covering all the samples. Oxygen in a higher concentration was only detected in the walls of the microspheres (**Figure 5c**), for all of the samples. In the case of the AlSi12 matrix larger areas of primer silicon were detected as expected. In the samples with the AlCu5 matrix copper-rich precipitations can be observed (with a dimension of approx. $1\ \mu\text{m} \times 20\ \mu\text{m}$ in **Figure 6**); according to the XRD measurements they are CuAl_2 particles. In the samples with the AlMgSi1 matrix magnesium showed a uniform

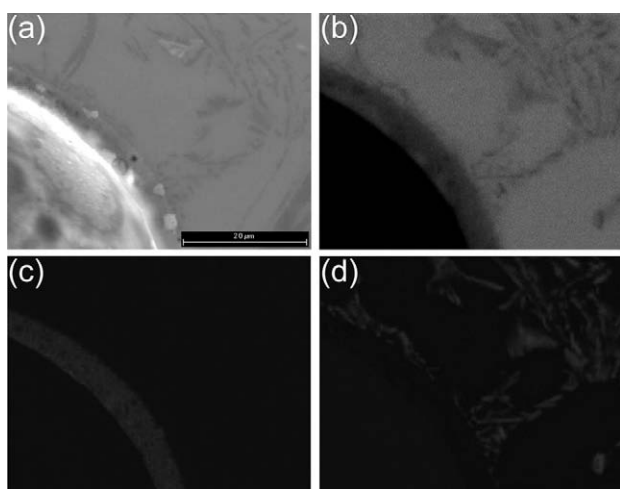


Figure 5: SEM image: a) from an Al99.5-matrix MMSF with an SL300-type microsphere and EDS maps of this area showing element distributions of: b) Al, c) O and d) Si

Slika 5: SEM-posnetek: a) Al99,5 MMSF osnove z SL300 mikrokroglico in EDS razporeditev elementov: b) Al, c) O in d) Si

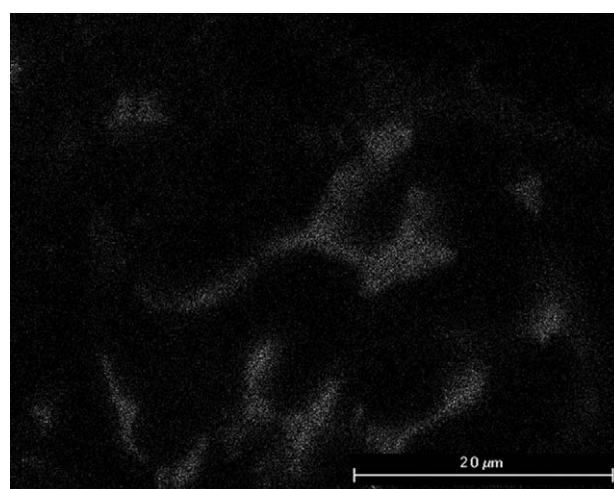


Figure 6: EDS map of an AlCu5-matrix MMSF with an SL150-type microsphere showing copper distribution and precipitations with the CuAl_2 phase

Slika 6: EDS-razporeditev bakra in izločki CuAl_2 faze v AlCu-osnovi MMSF z mikrokroglico SL150

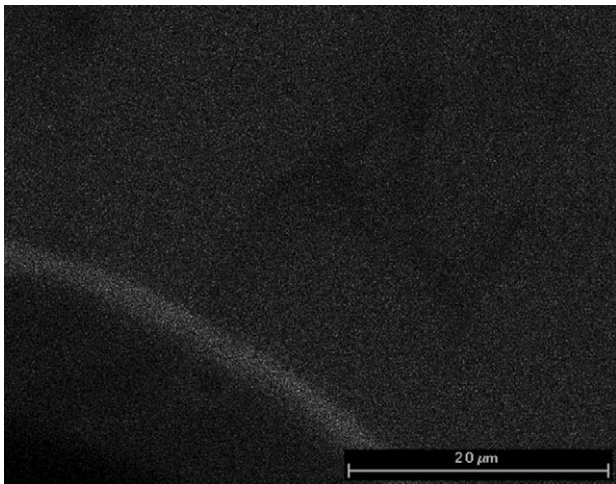


Figure 7: EDS map of an AlMgSi-matrix MMSF with an SL300-type microsphere showing Mg distribution and Mg enrichment in the microsphere's outer wall

Slika 7: EDS-razporeditev in obogatitev Mg v zunanji steni mikrokroglice v AlMgSi-osnovi MMSF z mikrokroglicami SL300

distribution in the aluminium areas, and no magnesium was detected in the primer silicon precipitations at all. Magnesium enrichment was detected alongside the microspheres' outer walls (Figure 7) indicating the solution of magnesium in the microspheres walls. For a more detailed investigation of the microsphere interface-matrix region, EDS line measurements were done at a higher resolution.

EDS line measurements were performed on polished specimens perpendicular to the interface layer between the microspheres and the matrix material. The interface layer is very important, because it is responsible for the load transfer from the matrix to the microspheres. The line-scan profiles showed the alternation of chemical elements along the line. The biggest advantage of the EDS line method is that it offers a very good opportunity to examine the interface layer and the changes in a hollow-microsphere wall in the matrix. Examples for the AlMgSi1 and the AlCu5 matrices are shown in Figures 8 and 9, respectively.

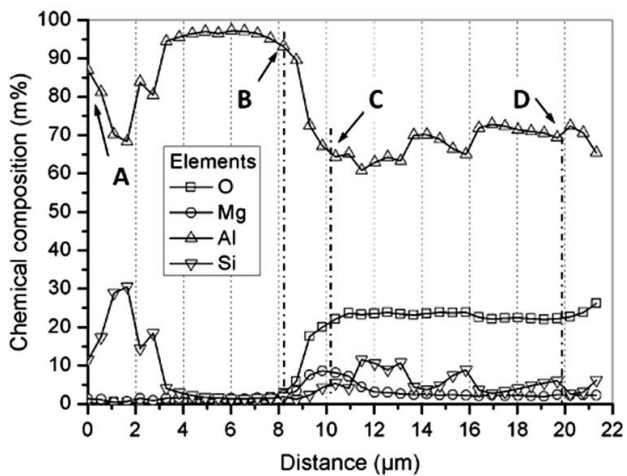
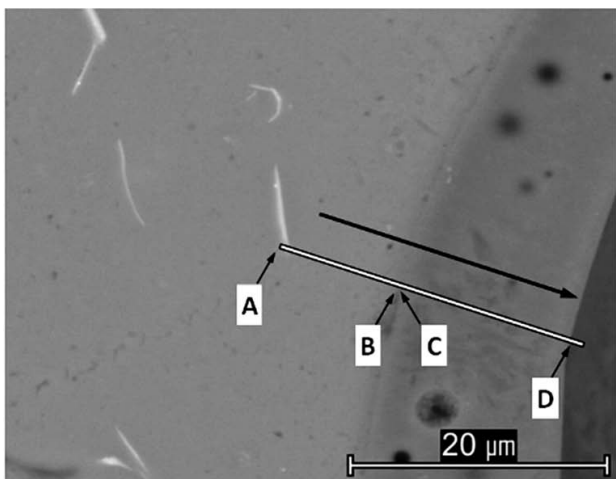


Figure 8: BSE image and EDS line-scan profiles of the AlMgSi-SL150 syntactic foam

Slika 8: BSE-posnetek in profil EDS-linjske analize pene, skladne z AlMgSi-SL50

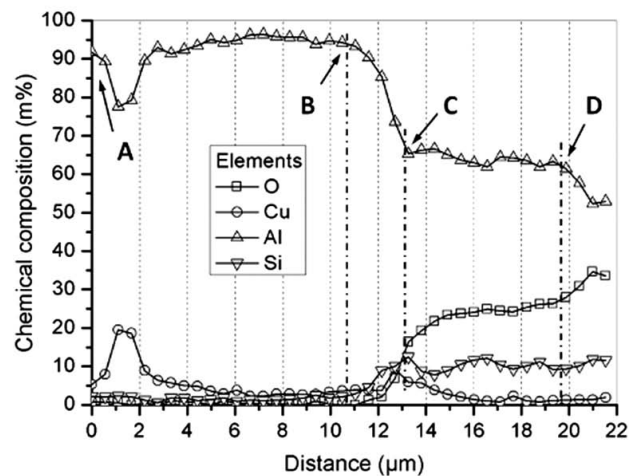
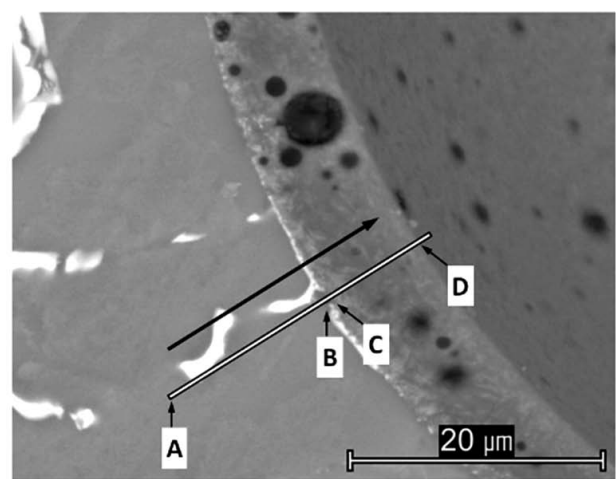


Figure 9: BSE image and EDS line-scan profiles of the AlCu5-SL300 syntactic foam

Slika 9: BSE-posnetek in profil EDS-linjske analize pene, skladne z AlCu5-SL300

In **Figure 8**, the wall of an SL150-type hollow microsphere can be observed in the high-magnification BSE image. It can be seen that the outer edge of the wall is not very well defined. This means that the surface of the microsphere is degraded. As mentioned above, the exchange reaction produces Al_2O_3 , which is advantageous, but not at the price of degrading the hollow microsphere's wall. The diffusion process made a relatively wide interface layer on the outer surface of the hollow microspheres (i.e. from point B to point C). The width of the interface layer was relatively wide $\approx 2\text{--}4\ \mu\text{m}$ (in previous research it was $6\ \mu\text{m}$ ²⁰) and it was measured between the significant changes of the derivation of the fitted curves showing the changing of the Al. Along the interface the Si and Al contents increased and decreased, respectively, with a moderate slope. After point C the Al content was alternated according to the actual composition of the wall. From point D the measurement is not reliable because of the curvature of the inner surface of the hollow microsphere.

In all of the aluminium and Al-alloy matrices the alternation of the Al and Si contents was observed because of the presence of the primer-Si precipitations in the alloy. In the case of the AlMgSi1 matrix (**Figure 8**) such primer-Si precipitation can be seen between points A and B. Points B and C were close to each other. This indicates that there is a very narrow (i.e. less than $3\ \mu\text{m}$) observable interface layer. In the concentration-sensitive BSE image, the lighter needle-like phases can be observed again in the walls of the SL150 spheres. The increase of the Mg content after point B confirms the presence of the magnesium solution in the microsphere wall, less than $4\ \mu\text{m}$ deep (this was also indicated by the EDS map measurements). In the case of the AlCu5 matrix (**Figure 9**) a precipitation (the CuAl_2 phase) can be observed between points A and B, while the interface layer was about $3\ \mu\text{m}$ on both SL150 and SL300 microspheres. Parts of the microspheres' walls were covered with the Cu precipitations, which can be clearly seen on the BSE image, but according to the EDS line measurements (between point B and C) this is not a solution in the microspheres' walls, but just a precipitation on them. In the case of the AlSi12 matrix the outer surface of the microsphere was seemingly unharmed as the exchange reaction was suppressed by the large Si content of the matrix. The interface layer was less than $1.5\ \mu\text{m}$ for both SL-type microspheres.

According to this, a well-defined Al and Si alternation occurred in the line of the EDS analysis diagram. In the lighter areas, the Si content decreased, while the Al content increased. There was no big fluctuation in the oxygen content within the matrix and within the microspheres' walls. This implies that, again, the lighter phases in the walls of the hollow microspheres are the Al_2O_3 particles embedded in the SiO_2 and mullite matrix. At point D, on the inner side of the hollow microsphere's wall, a very narrow Fe, Mg and K rich zone can be ob-

served (originated from the various oxides of the hollow microspheres).

Considering the possibility of chemical reactions between the microspheres and the matrix materials, it is worth mentioning that the ceramic microspheres can be used as a source of alloying elements in the MMSF systems. The appropriate choice and concentration of an alloying element in the wall material, or in the surface coating⁸ of the microspheres, can result in precipitation, grain refinement, and microstructure as per the designed scheme. These alloying elements can enhance the mechanical and/or other properties of the MMSFs. However, there is an effective range of the alloying elements due to the limited time after the infiltration and before the cooling. If the effective distance between the microspheres is small enough, it is possible to guarantee a homogenous microstructure. If the distance is larger, then the alloying effects are only in the vicinity of the microspheres.

To summarize, the EDS line measurements are applicable when investigating the interface layer between the microspheres and the matrix material. The investigations proved the presence of the Al_2O_3 needles in the walls and an exchange reaction between the SiO_2 content of the microsphere and the molten aluminium during the production. The suppressing effect of a high Si content was also confirmed. The alloying, or the coating, of the microspheres offers a great opportunity to influence the microstructure and the properties of MMSFs.

The authors assume that the microspheres also have an effect on the orientation and the size of the matrix-material grains. Therefore, the following paper will deal with the electron backscatter diffraction (EBSD) investigation of MMSFs.

4 CONCLUSIONS

From the results of the above mentioned and discussed EDS and XRD measurements, the following conclusions can be drawn:

The microstructures of the microspheres, their volume fraction and properties have a strong effect on the properties of MMSFs. The SEM and EDS investigations showed that Al_2O_3 needles can be found in the walls of the hollow ceramic microspheres. These needles are packed densely and they are embedded in the mixture of mullite and SiO_2 .

Due to the uneven distribution of Al_2O_3 , SiO_2 rich zones were formed on the surfaces of the microspheres. During the MMSF production the molten aluminium chemically attacked these zones and this reductive chemical reaction resulted in a severe damage of the microspheres' walls.

In the case of the Al99.5, AlCu5 and AlMgSi1 matrices the reaction was intensive. The driving force of the diffusion-controlled reaction was the Si concentration gradient between the microspheres and the matrix. In the

case of the AlSi12-matrix syntactic foams, the reaction was suppressed by a considerable amount of Si in the matrix alloy.

In the case of the AlCu5 matrix, local-copper precipitations were found on the microspheres' walls, while in the case of the AlMgSi1 matrix, magnesium was solved into the outer regions of the microspheres' walls.

In addition to the concrete conclusions above, it is worth mentioning that the ceramic microspheres can be used as a source of alloying elements in the MMSF systems. The appropriate choice and concentration of an alloying element in the wall material, or in a surface coating, of the microspheres can enhance the properties of MMSFs.

Acknowledgements

Special thanks to Professor J. T. Blucher for his kind support and to I. Sajó for XRD measurements. The Metal Matrix Composites Laboratory is supported by Grant # GVOP 3.2.1-2004-04-0145/3.0. This paper was supported by the János Bolyai Research Scholarship of the Hungarian Academy of Sciences. The investigations were supported by the Hungarian Research Fund, NKTH-OTKA PD 83687. This work is connected to the scientific programme of the "Development of quality-oriented and harmonized R+D+I strategy and functional model at BME" project. This project is supported by the New Széchenyi Plan (Project ID: TÁMOP-4.2.1/B-09/1/KMR-2010-0002).

5 REFERENCES

- ¹ N. Babcsán, D. Leitmeier, J. Banhart, *Colloids and Surfaces A: Physicochemical Engineering Aspects*, 261 (2005), 123–130
- ² N. Babcsán, F. García Moreno, J. Banhart, *Colloids and Surfaces A: Physicochemical Engineering Aspects*, 309 (2007), 254–263
- ³ I. N. Orbulov, J. Dobránszky, *Periodica Polytechnica Mechanical Engineering*, 52 (2008), 35–42
- ⁴ <http://www.envirospheres.com/products.asp>, 30. 11. 2011
- ⁵ <http://www.sphereservices.com/>, 30. 11. 2011
- ⁶ G. H. Wu, Z.Y. Dou, D. L. Sun, L. T. Jiang, B. S. Ding, B. F. He, *Scripta Materialia*, 56 (2007), 221–224
- ⁷ P. K. Rohatgi, J. K. Kim, N. Gupta, S. Alaraj, A. Daoud, *Composites Part A*, 27 (2006), 430–437
- ⁸ R. A. Palmer, K. Gao, T. M. Doan, L. Green, G. Cavallaro, *Materials Science and Engineering A*, 464 (2007), 85–92
- ⁹ D. K. Balch, J. G. O'Dwyer, G. R. Davis, C. M. Cady, G. T. Gray III, D. C. Dunand, *Materials Science and Engineering A*, 391 (2005), 408–417
- ¹⁰ W. J. Drury, S. A. Rickles, T. H. Sanders, J. K. Cochran: *Light weight alloys for aerospace applications*, The Minerals Metals and Materials Society, 1998, 311–322
- ¹¹ D. K. Balch, D. C. Dunand, *Acta Materialia*, 54 (2006), 1501–1511
- ¹² M. Ramachandra, K. Radhakrishna, *Journal of Materials Science*, 40 (2005), 5989–5997
- ¹³ M. Ramachandra, K. Radhakrishna, *Wear*, 262 (2007), 1450–1462
- ¹⁴ D. P. Mondal, J. Das, N. Jha, *Materials Design*, 30 (2008), 2563–2568
- ¹⁵ P. K. Rohatgi, R. Q. Guo, *Tribological Letters*, 3 (1997), 339–347
- ¹⁶ P. K. Rohatgi, R. Q. Guo, H. Iksan, E. J. Borchelt, R. Asthana, *Materials Science and Technology A*, 244 (1998), 22–30
- ¹⁷ T. Bárczy, Gy. Kaptay, *Materials Science Forum*, 473–474 (2005), 297–302
- ¹⁸ P. K. Trumble, *Acta Materialia*, 46 (1998), 2363–2367
- ¹⁹ I. N. Orbulov, Á. Németh, J. Dobránszky: *Hardness testing of metal matrix syntactic foams*, Proceedings of 7th International Conference on Mechanical Engineering, Budapest, Hungary, 2010, 16–22
- ²⁰ I. N. Orbulov, J. Dobránszky, Á. Németh, *Journal of Materials Science*, 44 (2009), 4013–4019